The Influence of N_7 Guanine Modifications on the Strength of Watson−Crick Base Pairing and Guanine N_1 Acidity: Comparison of Gas-Phase and Condensed-Phase Trends

Jaroslav V. Burda,*,† Jiří Šponer,*,‡,§ Jana Hrabáková,† Michal Zeizinger,† and Jerzy Leszczynski⊥

Department of Chemical Physics and Optics, Faculty of Mathematics and Physics, Charles University, Ke Karlovu 3, 121 16 Prague 2, Czech Republic, Institute of Biophysics, Academy of Sciences of the Czech Republic and National Center for Biomolecular Research, Kralovopolska 135, 612 65 Brno, Czech Republic, J. Heyrovský Institute of Physical Chemistry, Academy of Sciences of the Czech Republic, Dolejškova 3, 182 23 Prague 8, Czech Republic, and Department of Chemistry, Jackson State University, 1325 J. R. Lynch Street, Jackson, Mississippi 39217-0510

Received: December 30, 2002; In Final Form: February 27, 2003

Ab initio quantum-chemical calculations have been carried out to investigate the correlation between N_1-H_1 deprotonation energy and base pairing of modified guanines (neutral 8-oxoguanine (8OG) and monocationic 7,9-dimethylguanineH^+ (DMG)) and dicationic platinated guanines. The calculated intrinsic gas-phase trends are compared with available solution data. In the gas phase, the stability of the base pair increases with acidification of the $N_1(H_1)$ position; however, the relation is not linear. The guanine N_1 gas-phase deprotonation energies are primarily determined by the total charge of the system; however, there is also a nonnegligible contribution caused by polarization effects, which is especially significant for the DMG. The order of gas-phase deprotonation energies differs from solution pK_{a,H_2O} values. However, when assuming that the polar environment annihilates the ionic-electrostatic contribution, qualitative agreement is seen between the gas-phase and condensed-phase data. The pK_{a,H_2O} is primarily determined by polarization effects. In contrast, very poor correlation has been found between the intrinsic guanine−cytosine Watson−Crick (GC WC) base-pairing energies and the $K_{GC,DMSO}$ condensed-phase data, even when separately weighting the ionic-electrostatic and polarization contributions. The bell-shaped correlation between the solution N_1H acidity of the guanine derivative and the association constant K does not reflect the intrinsic gas-phase trends. The lack of correlation between gas-phase and solution data may be, for example, due to some specific interference with the GC WC base pairing caused by counteranions or presence of structures competing with the desired base pairing.

Introduction

Metal cations significantly influence the structure, dynamics, and function of DNA and RNA molecules. The metal cation−nucleic acids interactions range from nonspecific screening effects up to highly specific interactions with a binding of a given cation to a given site of the biomolecule.[1−8]

Recent advances of computational chemistry resulted in extensive applications of computational methods in studies on metal cation−nucleic acids interactions.[9−31] Because the interactions of metal cations are characterized by substantial polarization and charge-transfer effects, the applicability of simple pair-additive force fields is fundamentally limited. Thus, computational studies of metal binding to nucleic acids are often carried out using quantum-chemical methods. The quantum-chemical data are usually obtained for systems in complete isolation, that is, in the gas phase.

In the gas phase, the studied systems are dominated by the *ionic-electrostatic* contributions associated with the charge of the system. However, the ionic-electrostatic contributions are substantially affected (often canceled to large extent) by the solvent and counteranions in the bioinorganic experiments. The metal−cation binding is further associated with significant polarization and charge transfer contributions. Although their quantum-chemical origin comes from the Coulomb terms, these contributions are frequently quoted in the literature as *nonelectrostatic effects* to distinguish them from pair-additive long-range ionic-electrostatic contributions. The nonelectrostatic effects are essentially due to electron density redistribution and are much less affected by the environment screening.

The present paper compares the gas-phase and condensed-phase effects caused by guanine platination and modification on its base-pairing and acid−base properties. Comparison of gas-phase and solution trends improves our understanding of the molecular interactions and helps to separate the intrinsic properties of the studied systems from their interactions with the environment. Clear correlation between gas-phase and solution data indicates that the solution trends reflect the intrinsic properties of the metal−nucleobase interactions and the particular results likely can be extrapolated from one environment to another. In contrast, a lack of correlation indicates that the

* To whom correspondence should be addressed. E-mail addresses: burda@karlov.mff.cuni.cz; sponer@ibp.cz.

† Charles University.

‡ Institute of Biophysics, Academy of Sciences of the Czech Republic and National Center for Biomolecular Research.

§ J. Heyrovský Institute of Physical Chemistry, Academy of Sciences of the Czech Republic.

⊥ Jackson State University.

10.1021/jp027850g CCC: $25.00
Published on Web 05/10/2003

SCHEME 1

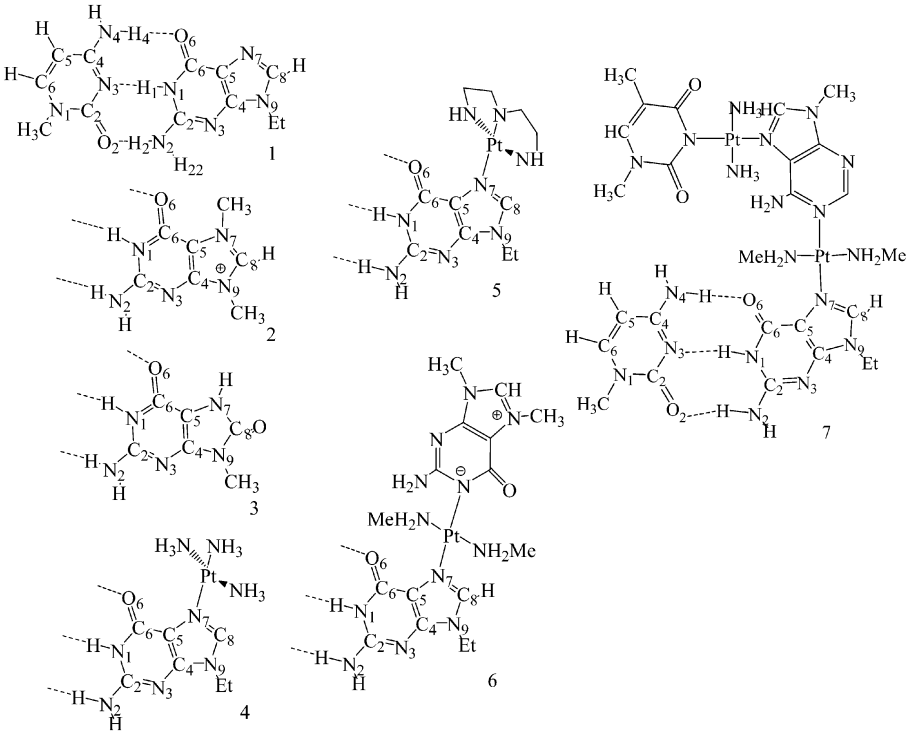

experimental outcome is substantially affected by the interactions of the studied systems with the environment and transferability of such results is not guaranteed. Notably, many experiments investigate small model systems similar to those studied by quantum mechanical (QM) computations, and some experiments are carried out in nonaqueous solutions, such as DMSO and $CDCl_3$.[1−3,6−8,24] Therefore, the experimental conditions often differ, and analysis of the intrinsic trends is thus vital.

In some cases, clear correlation between gas-phase and solution data was established. For example, intrinsic stability of base pairing is significantly enhanced because of polarization effects upon N_7 guanine metalation,[10,32] and this is also seen in solution.[33−35] Experiments reveal formation of metal-assisted nucleobase imino tautomers upon metal binding to the exocyclic amino groups of bases,[36−38] which can be fully explained as a result of intrinsic molecular-orbital effects caused by the cation binding.[39] QM calculations were also used to analyze the intrinsic properties of a *trans*-platinated base pair in solid state.[40] Interactions with the environment were shown to explain apparent disagreements between theoretical gas-phase and X-ray structures of Watson−Crick base pairs.[41] In contrast, the gas-phase protonation energies of metalated adenines are primarily determined by the charge of the metal adduct, while the corresponding aqueous solution pK_{a,H_2O} values are essentially independent of the charge. Still, when the ionic-electrostatic contribution is subtracted from the gas-phase data, qualitative correlation between gas-phase and solution data is achieved.[21] Relation between gas-phase and solution trends was also investigated for metal binding in proteins.[42−44]

The effects of metal binding and modifications on guanine base-pairing and acid−base properties are of interest for a number of reasons. Mutations caused by many metal species may be the result of nucleobase mispairing induced by alterations in acid−base properties of nucleobase atoms and groups involved in complementary H-bond formation. Monofunctional adducts (single-site binding) of a potent antitumor drug cisplatin cause mutations that appear to be independent of the primary cytotoxic effect caused mainly by intrastrand cross-link of two consecutive guanines.[45] Acidification of the N_1−H group of guanine would enhance the rate of a spontaneous proton transfer in the GC base pair and stabilize mismatched pairs. The same effect can be anticipated in case of *trans*-platin, which is tested in new generation of potential antisense drugs and efficiently stabilizes parallel-stranded DNA.[46,47] Platinum complexes with nucleobases may further be utilized to build up higher-order structures and supramolecular assemblies[8,48] in which the effects of metal binding on base-pairing and acid−base properties are of primary interest. For example, deprotonation of N_1 guanine position entirely changes its H-bonding properties and allows formation of triple-bonded guanine self-pairs. As part of the ongoing research in the field, the guanine−cytosine Watson−Crick (GC WC) base-pairing association constant K_{GC} in DMSO was recently correlated with N_1H acidity (pK_{a,H_2O}) in water for a set of modified and N_7-platinated guanines with varying charges (Scheme 1).[35] The experiments show initially a linear correlation; however, with further increase of the N_1H acidity, there is a spectacular drop of the base-pairing stability, resulting in a bell-shaped relation between $K_{GC,DMSO}$ and pK_{a,H_2O} (see Figure 8 in ref 35). This was tentatively explained as a result of significant reduction of H-bonding capability of O_6 upon excessive N_1 acidification, that is, by intrinsic properties of the nucleobases. In the present paper, we complement the experimental data using QM calculations and show, among other results, that the observed condensed-phase dependence cannot be explained on the basis of the intrinsic (gas-phase) deprotonation and base-pairing energies.

Computational Details

The hydrogen-bonding properties of 1-methylcytosine with the following guanine-base derivatives have been investigated (Scheme 1): 9-ethylguanine (labeled as structure **1** in Scheme 1 and abbreviated as 9EG throughout this paper), 7,9-dimethylguanineH^+ (DMG, structure **2**), and 8-oxo-9-methylguanine

(8OG, structure **3**), as well as four 9-ethylguanine complexes carrying different Pt(II) moieties at the N7 position, labeled P0G (structure **4**), P1G (structure **5**), P2G (structure **6**), and P3G (structure **7**). All of the complexes were preoptimized using the Hartree−Fock (HF) method in the minimal basis set (STO-3G) and then optimized with the more accurate 6-31G(d) basis set except for the largest complex (**7**), that is, P3GC. For the Pt atom description, the Stuttgart/Dresden relativistic energy-averaged small core pseudopotentials[49] were used. Final energy evaluation for the first six optimized complexes was done using the second-order Møller−Plesset (MP2) perturbation approach with the 6-31G(d) basis set. This computational level is similar to what has been used in many preceding studies of metal−nucleobase interaction and guarantees qualitatively correct results entirely sufficient for the purpose of this paper.[19−22,24] Specifically, the MP2//HF results do not qualitatively differ from DFT optimizations.[32,50] To further justify our results, we reinvestigated the three smallest systems also using the B3LYP/6-31G(d,p) method and RI-MP2 (resolution of identity MP2) procedure[51,52] with extended basis sets of atomic orbitals, as implemented in the Turbomole code.[53] The RI-MP2 method gives essentially identical results as the conventional MP2 but is considerably faster.[54]

The cytosine and guanine parts of the studied molecular complexes were also optimized in isolation. Then the (uncorrected) interaction energy between cytosine and the rest of the complex (the base-pairing energy), ΔE^{unc}, is evaluated as follows:

$$\Delta E^{\mathrm{unc}} = E_{\mathrm{compl}} - E_{\mathrm{G}}^{\mathrm{opt}} - E_{\mathrm{C}}^{\mathrm{opt}} \quad (1)$$

where E_{compl} is the MP2 energy of the optimized molecular complex while $E_{\mathrm{G}}^{\mathrm{opt}}$ and $E_{\mathrm{C}}^{\mathrm{opt}}$ are the MP2 energies of the optimized subsystems. Finally to obtain the true interaction energy ΔE, the basis set superposition error (BSSE) has to be eliminated using the counterpoise procedure. Thus, the interaction energy is calculated as follows:

$$\Delta E^{\mathrm{BSSE}} = E_{\mathrm{compl}} - E_{\mathrm{G}}^{\mathrm{ghost}} - E_{\mathrm{C}}^{\mathrm{ghost}} \quad (2)$$

where E_{compl} is the MP2 energy of the optimized molecular complex and $E_{\mathrm{G}}^{\mathrm{ghost}}$ ($E_{\mathrm{C}}^{\mathrm{ghost}}$) the MP2 energy of the guanine (cytosine) subsystem with its geometry taken from the optimized complex and with all dimer basis functions present (by "guanine subsystem" we mean the whole system without cytosine as seen in Scheme 1). The ΔE^{BSSE} values do not include the deformation energies of the monomers. These contributions need to be evaluated separately at the HF/6-31G(d) level that has been used for the optimizations.

An attempt was made for obtaining extrapolated data for the most extended P3GC complex, based on STO-3G optimizations and HF/6-31G(d) single-point calculations. The same calculations were tested also for all of the other complexes. However, comparing these geometries and pairing energies with MP2/6-31G(d)//HF/6-31G(d) data we concluded that the simplified procedure was not reliable enough. Thus, the P3G system was finally omitted from the discussion. Nevertheless, all of the data for system P3G appear to be similar to the other Pt-containing complexes and are thus not necessary for the following discussion.

Guanine N_1 gas-phase deprotonation energies were calculated in absence of the cytosine base as the electronic energy difference between optimized G and reoptimized structure of $G(-H_1)^-$ at the same level of theory (HF/6-31G(d)). To obtain better insight in the origin of variability of deprotonation energies, repulsion energy of H_1 from the rest of the system (neglecting the cytosine) was estimated using the classical electrostatic formula:

$$E^{\mathrm{rep}} = \frac{1}{4\pi\epsilon_0} \sum_{i \neq N_1} \frac{q_{H_1} q_i e^2}{r_{H_1 i}} \quad (3)$$

Parameters q_i were partial charges taken from NBO analysis. Interaction between the N_1 and H_1 atoms was omitted.

All calculations, except of the RI-MP2 data, were obtained with the Gaussian 98 code.[55]

TABLE 1: Base-Pairing Distances (Å)[a]

	C=O$_6$	N$_4$−H$_4$	O$_6$···H$_4$	N$_1$−H$_1$	H$_1$···N$_3$	C$_2$−N$_2$	N$_2$−H$_2$	H$_2$···O$_2$
GC	1.210	1.009	1.920	1.006	2.036	1.336	1.002	2.017
9EGC	1.211	1.008	1.920	1.008	2.042	1.337	1.002	2.005
DMGC	1.204	1.001	2.076	1.018	1.983	1.316	1.010	1.848
8OGC	1.219	1.008	1.929	1.010	2.017	1.334	1.003	1.991
P0GC	1.223	0.998	2.198	1.020	2.005	1.311	1.012	1.797
P1GC	1.223	0.998	2.193	1.019	2.015	1.312	1.011	1.808
P2GC	1.220	0.999	2.150	1.017	2.015	1.315	1.010	1.828

[a] Numbering of atoms is taken from Scheme 1.

TABLE 2: Pt(II) Coordination Parameters[a]

	Pt−N$_7$ (Å)	Pt−L$_2$ (Å)	Pt−L$_3$ (Å)	Pt−L$_4$ (Å)	torsion (deg)	H-bond (Å)
P0GC	2.052	2.123	2.085	2.112	−55.6	1.993
P1GC	2.067	2.057	2.076	2.118	−48.9	1.964
P2GC	2.074	2.091	2.086	2.108	−58.9	2.189

[a] L_3 is the cis-ligand H-bonded (see the last column) to the O_6 site of guanine, L_2 is the other cis-ligand, and L_4 is the trans-ligand to N_7 of guanine. Torsion angle is defined as $N(L_3)-Pt-N_7(G)-C_5(G)$.

Results and Discussion

Structures. The influence of guanine modifications and various platinum adducts on the geometry of GC base pair is summarized in Table 1. The table shows intermolecular distances and stretching of the covalent bonds involved in the pairing. The charge donation from different substituents (methyl-, ethyl-, oxo-, or platinum adducts) to guanine and the overall electrostatic field of the system have marked effect on the length of individual H-bonds. The electrostatic field of the positive charge localized around the guanine N_7 atom affects the position of the cytosine base because of interaction with the cytosine dipole moment and leads to counterrotation of the bases. The differences in the distributions of electron densities affect the H-bond lengths through changes of polarization and charge transfer. Typically, H_2 and H_1 hydrogens become more positive, and O_6 oxygen becomes less negative. The counterrotation of bases in the GC base pair has been documented in preceding studies and correlates with the charge of the system.[10,32] Upon neutralization, this geometrical effect is reduced; thus the geometry changes in DNA or RNA molecules are considerably smaller than those in the gas phase.[32]

The 9EGC system is basically equivalent to the unmodified GC base pair. The neutral 8OG derivate causes fairly small geometry changes. The monocationic DMG induces an apparent counterrotation of the bases that further increases for the 2+ Pt-adducts. Interestingly, the DMGC base pair shows the shortest sum of all three H-bond lengths. This indicates that the DMGC base pairing is accompanied by a relatively larger contribution of polarization effects to H-bonding compared to the other systems. The order of the $O_6\cdots H_4$ H-bond length is G = 9EG ≤ 8OG < DMG < P2G < P1G < P0G < P3G, while the

TABLE 3: Interaction Energies of the GC WC Base Pairing (ΔE(MP2)), HF-component of the Interaction Energies (ΔE(HF)), HF Deformation Energies of the Monomers (ΔE^{def}(HF)), Sum of ΔE(MP2) and ΔE^{def}(HF) (ΔE(GC)), $H_1(N_1)$ Guanine Deprotonation Energies (ΔE^{deprot}), and Aqueous Solution Experimental pK_{a,H_2O} Values in Water and DMSO Association Constants

	ΔE(MP2)[b]	ΔE(HF)	ΔE^{def}(HF)	ΔE(GC)	ΔE^{deprot}	pK_{a,H_2O}[d]	$K_{GC/DMSO}$ (expt[d])
9EGC	−26.24 (−31.09)[c]	−15.55	−2.58	−23.66	352.46	9.54	6.9
DMGC	−35.89 (−41.66)	−25.07	−2.13	−33.76	262.87	7.27	8.8
8OGC	−26.95 (−22.49)	−17.78	−1.80	−25.15	345.14	8.77	12.6
P0GC	−38.04 (−44.14)	−28.79	−2.19	−35.85	204.91		
P1GC	−36.23 (−42.38)	−30.78	−2.15	−34.08	210.72	8.14	13.0
P2GC	−34.58 (−40.74)	−24.48	−2.39	−32.19	218.50	8.23	22 ± 10

[a] All data are in kcal/mol. [b] Values in parentheses are without the BSSE correction. [c] MP2 results for GC base pair are −26.30 kcal/mol, taken from ref 9. [d] Experimental values are taken from ref 35.

reversed order is seen for the $H_2\cdots O_2$ H-bond. The length of the middle bond shows the trend DMG < P0G = P3G < P1G = P2G = 8OG < G < 9EG, but the differences are smaller (within 0.06Å) in comparison with $O_6\cdots H_4$ (0.28 Å) and $H_2\cdots O_2$ (0.22 Å) distance variations. The shifts of electron densities have marked effect on the N_1-H_1 bond length. Extension of the N−H bond is clearly correlated with the strength of the H-bonding, namely, the strengthening via the guanine polarization. Note that the DMG derivate with charge of +1 causes a similar N−H stretching as the Pt-adducts with charges +2. An analogous trend is seen for the N_2-H_2 bond, while the cytosine N_4-H_4 bond shows the reverse trend.

Table 2 shows bond lengths between coordinated nitrogens and the central Pt atom. It was reported earlier[56] that ammonium has smaller trans effect due to its inability of back-donation. It represents relatively weak competition compared to guanine, and it results in the strongest $Pt-N_7$ interaction in P0G derivate. Corresponding characteristics—the shortest $Pt-N_7$ distance (2.052 Å) and relatively long $Pt-L_4$ bond from the trans site of square planar Pt(II) arrangement are apparent. The longest Pt−N bond occurs also in this complex: $Pt-L_2$; L_2 is the ammonium ligand in trans position to NH_3 that forms a H-bond to the O_6 site of guanine. Here, smaller screening of the N atom by its hydrogens leads to a firmer Pt−N bond (2.085Å), pushing the opposite ligand further away from Pt.

The 1,5-diaminepentan-3-azo ligand of P1G partially resembles the bonding condition of the P0G complex with three ammonia (poor back-donation capability), and similarly strong $Pt-N_7$ coordination is observed. In the case of P2G structure, the Pt adduct with another guanine coordinated through its N_1 site leads to a complex that resembles a Hoogsteen GG pair mediated by platinum instead of H-bonding. A stronger dative $Pt-N_1$ bond (2.091Å) leads to a weaker $Pt-N_7$ interaction with a somewhat larger distance (2.074Å). On the basis of the trial calculations (see method), it seems that P3G should lead to a similar bonding and energetic distribution as P2G.

Gas-Phase Interaction Energies and Deprotonation Energies. Table 3 collects the gas-phase deprotonation and interaction energies, together with the experimental pK_{a,H_2O} and $K_{GC,DMSO}$ values. The neutral systems have very similar pairing energies, essentially identical to unmodified GC base pair. However, 8OG is characterized by a ca. 7 kcal/mol drop in the deprotonation energy compared to 9EG.

The monocationic DMG shows a substantial increase of base-pairing stability by ca. 10 kcal/mol compared with the neutral systems. It also causes a ca. 90 kcal/mol drop of the deprotonation energy. The dicationic Pt adducts provide similar enhancement of base pairing as DMG; however, they cause a substantial additional reduction of the deprotonation energies in the range of 40−55 kcal/mol with respect to DMG. This nevertheless is a considerably smaller difference compared to that of 90 kcal/mol between neutral 9EG and monocationic DMG.

TABLE 4: NBO Partial Charges on Selected Atoms of Studied Complexes[a]

	GC	9EGC	DMGC	8OGC	P0GC	P1GC	P2GC
total	0	0	1	0	2	2	2
N_7(gua)	−0.450	−0.457	−0.288	−0.619	−0.501	−0.503	−0.502
N_9	−0.568	−0.394	−0.333	−0.453	−0.338	−0.336	−0.343
C_8	0.185	0.194	0.256	0.800	0.222	0.236	0.232
H_8/O_8	0.221	0.214	0.260	−0.668	0.248	0.256	0.257
O_6	−0.635	−0.641	−0.606	−0.675	−0.678	−0.625	−0.612
N_1	−0.650	−0.649	−0.636	−0.634	−0.620	−0.625	−0.632
H_1	0.454	0.453	0.472	0.456	0.476	0.455	0.451
C_2	0.628	0.635	0.651	0.633	0.647	0.648	0.646
N_2	−0.837	−0.837	−0.787	−0.832	−0.775	−0.795	−0.801
H_2	0.439	0.438	0.453	0.439	0.456	0.434	0.431
H_{22}	0.421	0.419	0.435	0.422	0.441	0.454	0.451
N_3	−0.587	−0.602	−0.584	−0.585	−0.568	−0.557	−0.562
N_1(cyt)	−0.616	−0.435	−0.424	−0.434	−0.417		
O_2	−0.653	−0.665	−0.677	−0.665	−0.675		
N_3	−0.637	−0.636	−0.649	−0.638	−0.652		
N_4	−0.779	−0.781	−0.783	−0.782	−0.796		
H_4	0.452	0.450	0.438	0.449	0.428		
Pt					0.673	0.642	0.656
$N(L_2)$[b]					−1.032	−0.839	−0.812
$N(L_3)$[b]					−1.019	−0.823	−0.806
$N(L_4)$[b]					−1.040	−0.630	−0.645

[a] Numbering of atoms is taken from Scheme 1, and the ligands are marked according to Table 2. [b] L_3 is the cis-ligand H-bonded (see the last column) to the O_6 site of guanine, L_2 is the other cis-ligand, and L_4 is the trans-ligand to N_7 of guanine. Torsion angle is defined as $N(L_3)-Pt-N_7(G)-C_5(G)$..

It is known that the enhancement of base pairing of the GC base pair upon N_7 cation binding is mostly of a polarization origin,[9,10] while gas-phase deprotonation energies of nucleobases are primarily due to the long-range ionic-electrostatic effects further modulated by electron density shifts.[21,39] Thus, the GC interaction and deprotonation energies suggest that the DMG modification is associated with more pronounced polarization effects compared to the $Pt-N_7$ binding, especially considering that DMG is a monocation. This is in line with the geometry analysis presented above.

Charge Distribution. NBO partial charges on selected atoms of guanine, cytosine, and the Pt adducts are depicted in Table 4. Partial charges on guanine atoms in the 9EG structure resemble the electron distribution of the isolated GC pair with the only exception of N_9. A higher charge on N_1 of cytosine is related to the different N_1 substituent (H vs methyl group). Electron distribution of 8OG system differs more substantially, but similarity still can be found in the H-bond region (especially partial charges on H_1, N_2, H_2, and also on selected atoms of cytosine). This explains similarity in their H-bonding. Figure 1 demonstrates the electrostatic repulsion of the H_1 hydrogen from

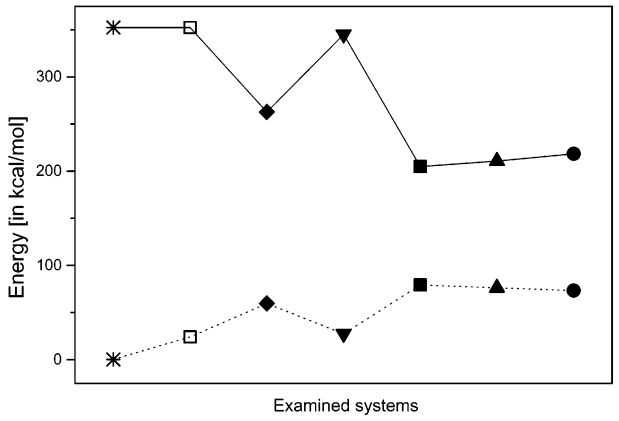

Figure 1. Comparison of H_1 deprotonation energies (solid line) and electrostatic repulsions between the H_1 atom and the rest of the system calculated using eq 3 (dotted line): (∗) GC, (□) 9EGC, (◆) DMGC, (▼) 8OGC, (■) P0GC, (▲) P1GC, (●) P2GC.

the rest of the system estimated using eq 3 and the above charge distribution. There is a clear correlation between the electrostatic repulsion and the H_1 destabilization.

The electron density shifts show interesting variability for different systems. Positively charged metals interact with the N_7 position and thus cause a rather "diagonal" density shift in the direction of N_7-N_2. However, in the DMG, the positive total charge is distributed over the whole guanine fairly proportionally, decreasing (in absolute value) negative and increasing positive partial charges of individual atoms. This leads to stronger H-bonds involving (more positive) hydrogens and weaker H-bonds involving the (less negative) O_6 atom of guanine. This trend actually appears to concur with the suggestion by Sigel et al.[35] regarding a destabilization of the $O_6\cdots N_4$ H-bond in the case of DMG. As it was shown above, however, the $O_6\cdots N_4$ H-bond destabilization is counterbalanced by strengthening of the other H-bonds. The electron density shifts and the structural data suggest that DMG affects base pairing by a different mechanism compared with the platinated species: the charge distribution of the six-membered ring of DMG and Pt-G is similar, despite the different origin of DMG modification in comparison with platinum adducts; however, there is an apparent difference on the five-membered ring caused by the increase of electron density due to metal induction for Pt complexes on one side and reduction of electron density due to the total +1 charge on DMG on other side.

Gas-Phase vs Condensed-Phase Trends. Figure 2 shows the correlation between the gas-phase base-pairing energy and the gas-phase deprotonation energy of the N_1 guanine position. The relation is not linear. Stability of the 7,9-dimethyl-$GH^+\cdot C$ base pair is considerably larger than one would expect from a linear interpolation between neutral and +2 charged PtG systems. The deviation for DMG occurs in the *opposite direction* compared to the parabolic trend reported by Sigel et al in their solution experiment.[35] In fact, however, we do not assume that the parabolic trend seen in the present set of systems reveals any general relation between gas-phase base-pairing and deprotonation energies. The DMG system shows a different balance of electrostatic and polarization effects compared to the Pt systems, causing the apparent nonlinearity of the correlation.

Finally, let us compare the gas-phase data with the solution experiments. Figure 3 shows the correlation between the gas-phase deprotonation energy and the pK_{a,H_2O} values. While in the gas phase, the +2 Pt systems show the largest destabilization of the $H_1(N_1)$; in a water environment, the DMG shows the most pronounced N_1 acidification. This marked difference can

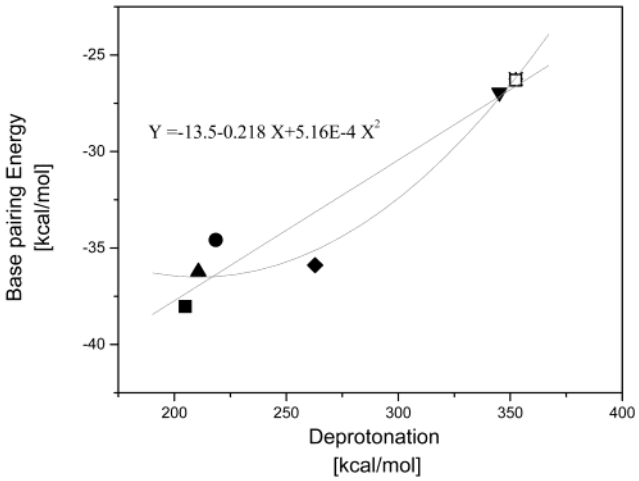

Figure 2. Correlation between calculated deprotonation energy and base-pair GC interaction energy in the gas phase: (∗) GC, (□) 9EGC, (◆) DMGC, (▼) 8OGC, (■) P0GC, (▲) P1GC, (●) P2GC. Note that the parabolic dependence is indicated solely to demonstrate its opposite direction compared to the condensed-phase data (see the text).

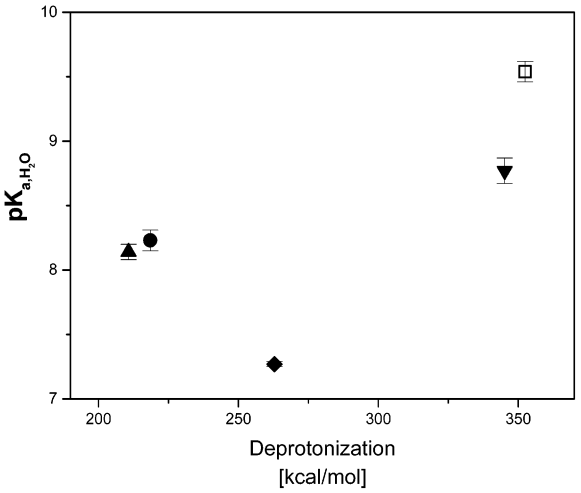

Figure 3. Comparison of gas-phase deprotonation energies with the corresponding pK_{a,H_2O} condensed phase values: (□) 9EGC, (◆) DMGC, (▼) 8OGC, (▲) P1GC, (●) P2GC. pK_{a,H_2O} error bars are taken from ref 35.

be explained in the following way. The gas-phase deprotonation energy is dominated by the ionic-electrostatic effect and only partly modulated by the electron density distribution changes. In aqueous solution, the role of the ionic-electrostatic term is substantially reduced (basically annihilated) and the dependence is then dominated by the density distribution changes that should not be markedly influenced by the solvent. Thus, the gas-phase drop in deprotonation energy of ca. 8 kcal/mol between guanine and 8OG is reflected by the ca. 0.8 log unit change of pK_{a,H_2O}. Because both systems are neutral, we essentially see the net effect of electronic structure differences, which is not affected by the solvent screening. Platination leads to a further ca. 0.5 log unit drop of pK_{a,H_2O}. This is of course a much smaller effect than that in the gas phase, and it is due to the screening of the leading ionic-electrostatic term in water. Finally, the DMG causes a further drop of pK_{a,H_2O} by ca. 1 log unit, deviating thus completely from the gas-phase trend. However, the result can be well understood because (see above) the electron density of DMG exhibits, among the studied systems, the largest redistribution in comparison with the unmodified guanine base. Because aqueous solution data reflect primarily this nonelectrostatic term, the DMG shows the largest acidification. Thus

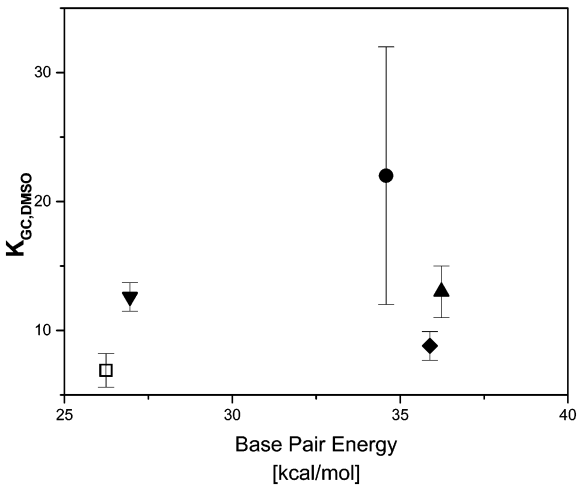

Figure 4. Comparison of gas-phase base-pair interaction energies with stability constants in condensed phase (DMSO): (□) 9EGC, (◆) DMGC, (▼) 8OGC, (▲) P1GC, (●) P2GC. Error bars taken from ref 35.

the gas-phase and aqueous-solution data can be well correlated under the assumption that the ionic-electrostatic effects are essentially eliminated by the solvent and the pK_{a,H_2O} changes are caused by the nonelectrostatic (polarization) contributions. This finding agrees with our preceding studies of platinated adenines and metal-assisted nucleobase tautomers.[21,39]

Figure 4 shows that there is no correlation between the gas-phase interaction energy and the base-pair stability in DMSO. The Pt-GC base pairs show enhanced stability in gas phase and in solution with respect to the reference 9EGC system. The condensed-phase data, however, also reveal a rather significant stabilization of the base pairing of 8OG relative to that of 9EG, while both base pairs are nearly isoenergetic in the gas phase. The most striking example is the DMGC base pair. Its rather low stability in DMSO contrasts with the sharply increased stability in the gas phase. In addition, as we have argued above, the strong stabilization of DMGC base pair in the gas phase is primarily due to a profound electron distribution shift. Such polarization (nonelectrostatic) effect should not be significantly affected by nonspecific (continuum) solvent screening. In conclusion, the $K_{GC,DMSO}$ data does not correlate with the intrinsic gas-phase trends even when separately considering the ionic-electrostatic and polarization effects.

Accuracy of the Results. It is to be noted that the above-reported trends are not substantially affected by accuracy of either the experiments or the computations. Error bars of the pK_{a,H_2O} measurements are very small, and the same is true also for the solution association constants, except those of the P2GC pair. However, the main conclusions remain unchanged even when the P2GC data is not considered. The QM calculations are fairly accurate. We used the MP2//HF method extensively in the past for metal−base-pair interactions, and the results were similar to those obtained by DFT.[19] Similar conclusions for some related systems can be found in studies performed by other researchers.[42,57−61] The present calculations systematically underestimate the absolute gas-phase binding energies of base pairs by a few kilocalories per mole because of incomplete inclusion of intermolecular electron correlation energy.[62] The relative order of stability is predicted with an uncertainty of ca. 2 kcal/mol or better over the whole range of possible pairing patterns.

Nevertheless, on the basis of the referee's suggestions, we carried out additional reference calculations. Because the Pt-containing systems are too large, we considered only the G, 8OG, and DMG molecules. At the B3LYP/6-31G(d,p)//B3LYP/6-31G(d,p) level, the interaction energies with inclusion of monomer deformations are −25.25, −24.98, and −35.82 kcal/mol for GC, 8OGC, and DMGC base pairs, respectively. Because the GC and 8OGC base pairs are close to each other in energy, we carried out very accurate RI-MP2/aug-cc-pVTZ//RI-MP2/cc-pVTZ calculations. The corresponding interaction energies with inclusion of monomer deformations are −26.76 and −27.21 kcal/mol for GC and 8OGC. Thus, the stabilization is modestly improved, as expected, but especially, the relative changes are too small to affect any of the conclusions of the present paper. Regarding the deprotonation energies, the B3LYP/6-31G(d,p) method provides values of 356.8, 350.6, and 266.9 kcal/mol for G, 8OG and DMG, respectively, while the most accurate MP2/cc-pVTZ values are 346.5, 337.6, and 256.5 kcal/mol. Thus there is a small variability of the absolute values with no significant changes of the relative trends.

Concluding Remarks

Gas-phase deprotonation energies of guanine N_1-H_1 position and its base-pairing energies with cytosine were compared for a series of modified and N_7-platinated guanines with charges ranging from 0 to +2. The gas-phase data were correlated with available condensed-phase experiments.

In the gas phase, the stability of the base pair increases with acidification of the N_1 position. However, the relation is not entirely linear. The guanine N_1 deprotonation energies are primarily determined by ionic-electrostatic interactions associated with the total charge of the system. Nevertheless, there is also a nonnegligible contribution caused by polarization effects, which is especially significant for 7,9-dimethylguanineH^+. The improvement of GC base pairing caused by metalation and modification of guanine is primarily caused by polarization effects.

The order of gas-phase deprotonation energies differs significantly from the available solution pK_{a,H_2O} values. However, when one assumes that the polar environment substantially reduces or annihilates the ionic-electrostatic effects, qualitative agreement between the gas-phase and condensed-phase data is seen. The same conclusion was reached when comparing solution and gas-phase data for protonation of metalated adenines.[21]

In contrast, poor correlation was found between the intrinsic gas-phase GC WC base-pairing energies and the $K_{GC,DMSO}$ condensed-phase data. Agreement was not achieved even when separately weighting the electrostatic and polarization contributions. The differences are significant and can be explained neither by the error margins of experiment nor by accuracy of the calculations. The most striking example is the 7,9-dimethylguanineH^+·C base pair. This base pair has rather low stability in DMSO, which sharply contrasts its large stability in the gas phase. Thus, the parabolic shape of the $K_{GC,DMSO}$ vs pK_{a,H_2O} dependence suggested by recent experiments does not originate in the intrinsic properties of the studied systems. It indicates that the outcome of the measurement might be affected by some specific interactions with the environment, contacts with counteranions present in solution, presence of undetected structures competing with the desired base pairing, etc. Note that such a very specific interaction was recently suggested to the explain unexpected lack of base pairing of N_1-platinated adenine and thymine in $CDCl_3$.[24] In that particular case, nitrate counteranions interacting with the Pt adduct probably prevented the expected Hoogsteen base pairing despite that the platination

itself intrinsically modestly supports the base pairing. Thus, the QM calculations have a rather limited capability to predict solution association constants of modified/metalated nucleobases, while the solution experiments do not unambiguously reflect the intrinsic stability of the base pairs and the stability order may be different in different environments. The present paper demonstrates that computational and experimental[63−74] gas-phase studies on various aspects of nucleobase properties and interactions provide useful information complementing the condensed-phase and solid-state experimental data.

Acknowledgment. This study was supported by Charles University Grants GAUK 181/2002/B_FYZ/MFF (J.V.B.) and 259/2002/B_CH/MFF (M.Z.), Grant NSF-MSMT ME 517 (J.V.B.), Grant LN00A016 by Ministry of Education of the Czech Republic (J.S.), Senior Wellcome Trust Fellowship for Biomedical Research in Central Europe Grant GR067507MF (J.S.), Grant ONR N00034-03-1-0116 (J.L.), and Grant NSF-CREST No. 9805465 (J.L.). We thank Meta-Centers in Prague (Charles University and Technical University), Brno (Masaryk University), and Pilsen (West Bohemia University) for the generous support of the computational resources and kindly understanding.

References and Notes

(1) *Metal Ions in Genetic Information Transfer*; Elsevier: New York, 1981; Vol. 3.

(2) *Interactions of Metal Ions with Nucleotides, Nucleic Acids and Their Constituents*; Marcel Dekker: New York, 1996; Vol. 32.

(3) *Probing of Nucleic Acids by Metal Ion Complexes of Small Molecules*; Marcel Dekker: New York, 1996; Vol. 33.

(4) Pyle, A. M.; Barton, J. K. *Prog. Inorg. Chem.* **1990**, *38*, 413−475.

(5) Martin, R. B. *Acc. Chem. Res.* **1985**, *18*, 32−38.

(6) Lippert, B. *Prog. Inorg. Chem.* **1989**, *37*, 1−9.

(7) Lippert, B. *Coord. Chem. Rev.* **2000**, *200*, 487−516.

(8) Houlton, A. *Adv. Inorg. Chem.* **2002**, *53*, 87−158.

(9) Burda, J. V.; Šponer, J.; Leszczynski, J.; Hobza, P. *J. Phys. Chem. B* **1997**, *101*, 9670−9677.

(10) Šponer, J.; Burda, J. V.; Sabat, M.; Leszczynski, J.; Hobza, P. *J. Phys. Chem. A* **1998**, *102*, 5951−5957.

(11) Munoz, J.; Gelpi, J. L.; Soler-Lopez, M.; Subirana, J. A.; Orozco, M.; Luque, F. J. *J. Phys. Chem. B* **2002**, *106*, 8849−8857.

(12) Meyer, M.; Steinke, T.; Brandl, M.; Suhnel, J. *J. Comput. Chem.* **2001**, *22*, 109−124.

(13) Famulari, A.; Moroni, F.; Sironi, M.; Gianinetti, E.; Raimondi, M. *J. Mol. Struct. (THEOCHEM)* **2000**, *529*, 209−217.

(14) Pelmenschikov, A.; Zilberberg, I.; Leszczynski, J.; Famulari, A.; Sironi, M.; Raimondi, M. *Chem. Phys. Lett.* **1999**, *314*, 496−500.

(15) Carloni, P.; Sprik, M.; Andreoni, W. *J. Phys. Chem. B* **2000**, *104*, 823−835.

(16) Petrov, A. S.; Lamm, G.; Pack, G. R. *J. Phys. Chem. B* **2002**, *106*, 3294−3300.

(17) Russo, N.; Toscano, M.; Grand, A. *J. Am. Chem. Soc.* **2001**, *123*, 10272−10279.

(18) Luna, A.; Gevrey, S.; Tortajada, J. *J. Phys. Chem. B* **2000**, *104*, 110−118.

(19) Burda, J. V.; Šponer, J.; Leszczynski, J. *Phys. Chem. Chem. Phys.* **2001**, *3*, 4404−4411.

(20) Burda, J. V.; Šponer, J.; Leszczynski, J. *J. Biol. Inorg. Chem.* **2000**, *5*, 178−188.

(21) Šponer, J. E.; Leszczynski, J.; Glahe, F.; Lippert, B.; Šponer, J. *Inorg. Chem.* **2001**, *40*, 3269−3278.

(22) Deubel, D. V. *J. Am. Chem. Soc.* **2002**, *124*, 5834−5842.

(23) Baik, M. H.; Friesner, R. A.; Lippard, S. J. *J. Am. Chem. Soc.* **2002**, *124*, 4495−4503.

(24) Schmidt, K. S.; Reedijk, J.; Weisz, K.; Janke, E. M. B.; Sponer, J. E.; Sponer, J.; Lippert, B. *Inorg. Chem.* **2002**, *41*, 2855−2863.

(25) Stewart, G. M.; Tiekink, E. R. T.; Buntine, M. A. *J. Phys. Chem. A* **1997**, *101*, 5368−5373.

(26) Martinez, J. M.; Elmroth, S. K. C.; Kloo, L. *J. Am. Chem. Soc.* **2001**, *123*, 12279−12289.

(27) Špaèková, N.; Berger, I.; Šponer, J. *J. Am. Chem. Soc.* **1999**, *121*, 5519−5534.

(28) Elizondo-Riojas, M. A.; Kozelka, J. *J. Mol. Biol.* **2001**, *314*, 1227−1243.

(29) Beveridge, D. L.; McConnell, K. J. *Curr. Opin. Struct. Biol.* **2000**, *10*, 182−196.

(30) Gresh, N.; Policar, C.; Giessner-Prettre, C. *J. Phys. Chem. B* **2002**, *106*, 11A-11A.

(31) Garmer, D. R.; Gresh, N.; Roques, B. P. *Proteins Struct. Funct. Genet.* **1998**, *31*, 42−60.

(32) Šponer, J.; Sabat, M.; Gorb, L.; Leszczynski, J.; Lippert, B.; Hobza, P. *J. Phys. Chem. B* **2000**, *104*, 7535−7544.

(33) Bruning, W.; Sigel, R. K. O.; Freisinger, E.; Lippert, B. *Angew. Chem., Int. Ed.* **2001**, *40*, 3397.

(34) Sigel, R. K. O.; Lippert, B. *Chem. Commun.* **1999**, 2167.

(35) Sigel, R. K. O.; Freisinger, E.; Lippert, B. *J. Biol. Inorg. Chem.* **2000**, *5*, 287−299.

(36) Lippert, B.; Schollhorn, H.; Thewalt, U. *J. Am. Chem. Soc.* **1986**, *108*, 6616−6621.

(37) Zamora, F.; Kunsman, M.; Sabat, M.; Lippert, B. *Inorg. Chem.* **1997**, *36*, 1583−1587.

(38) Velders, A. H.; van der Geest, B.; Kooijman, H.; Spek, A. L.; Haasnoot, J. G.; Reedijk, J. *Eur. J. Inorg. Chem.* **2001**, *2*, 369−372.

(39) Šponer, J.; Šponer, J. E.; Gorb, L.; Leszczynski, J.; Lippert, B. *J. Phys. Chem. A* **1999**, *103*, 11406−11413.

(40) Carloni, P.; Andreoni, W. *J. Phys. Chem.* **1996**, *100*, 17797−17800.

(41) Guerra, C. F.; Bickelhaupt, F. M.; Snijders, J. G.; Baerends, E. J. *J. Am. Chem. Soc.* **2000**, *122*, 4117−4128.

(42) Rulí×f0ek, L.; Havlas, Z. *J. Am. Chem. Soc.* **2000**, *122*, 10428−10439.

(43) Dudev, T.; Lim, C. *J. Am. Chem. Soc.* **2002**, *124*, 6759−6766.

(44) Ryde, U.; Olsen, L.; Nilsson, K. *J. Comput. Chem.* **2002**, *23*, 1058−1070.

(45) Lippert, B. *Cisplatin: Chemistry and Biochemistry of a leading anticancer drug.*; Wiley-VCH: Wienheim, Germany, 1999.

(46) Schmidt, K. S.; Boudvillain, M.; Schwartz, A.; van der Marel, G. A.; van Boom, J. H.; Reedijk, J.; Lippert, B. *Chem.—Eur. J.* **2002**, *8*, 5566−5570.

(47) Muller, J.; Drumm, M.; Boudvillain, M.; Leng, M.; Sletten, E.; Lippert, B. *J. Biol. Inorg. Chem.* **2000**, *5*, 603−611.

(48) Navarro, J. A. R.; Lippert, B. *Coord. Chem. Rev.* **2001**, *222*, 219−250.

(49) Dolg, M.; Stoll, H.; Preuss, H.; Pitzer, R. M. *J. Phys. Chem.* **1993**, *97*, 5852.

(50) Rulisek, L.; Šponer, J. *J. Phys. Chem. B*, in press.

(51) Weigend, F.; Haser, M. *Theor. Chem. Acc.* **1997**, *97*, 331−340.

(52) Weigend, F.; Haeser, M.; Patzelt, H.; Ahlrichs, R. *Chem. Phys. Lett.* **1998**, *294*, 143−152.

(53) Ahlrichs, R.; Bar, M.; Haser, M.; Horn, H.; Kolmel, C. *Chem. Phys. Lett.* **1989**, *162*, 165−169.

(54) Jurecka, P.; Nachtigall, P.; Hobza, P. *Phys. Chem. Chem. Phys.* **2001**, *3*, 4578−4582.

(55) Frisch, M. J.; Trucks, G. W.; Schlegel, H. B.; Scuseria, G. E.; Robb, M. A.; Cheeseman, J. R.; Zakrzewski, V. G.; Montgomery, J. A., Jr.; Stratmann, R. E.; Burant, J. C.; Dapprich, S.; Millam, J. M.; Daniels, A. D.; Kudin, K. N.; Strain, M. C.; Farkas, O.; Tomasi, J.; Barone, V.; Cossi, M.; Cammi, R.; Mennucci, B.; Pomelli, C.; Adamo, C.; Clifford, S.; Ochterski, J.; Petersson, G. A.; Ayala, P. Y.; Cui, Q.; Morokuma, K.; Malick, D. K.; Rabuck, A. D.; Raghavachari, K.; Foresman, J. B.; Cioslowski, J.; Ortiz, J. V.; Stefanov, B. B.; Liu, G.; Liashenko, A.; Piskorz, P.; Komaromi, I.; Gomperts, R.; Martin, R. L.; Fox, D. J.; Keith, T.; Al-Laham, M. A.; Peng, C. Y.; Nanayakkara, A.; Gonzalez, C.; Challacombe, M.; Gill, P. M. W.; Johnson, B. G.; Chen, W.; Wong, M. W.; Andres, J. L.; Head-Gordon, M.; Replogle, E. S.; Pople, J. A. *Gaussian 98*, revision A.1x; Gaussian, Inc.: Pittsburgh, PA, 1998.

(56) Burda, J. V.; Leszczynski, J., submitted for publication.

(57) Blomberg, M.; Yi, S. S.; Noll, R. J.; Weisshaar, J. C. *J. Phys. Chem. A* **1999**, *103*, 7254−7267.

(58) Bridgeman, A. J.; Cavigliasso, G.; Harris, N.; Young, N. A. *Chem. Phys. Lett.* **2002**, *351*, 319−326.

(59) Broo, A.; Holmen, A. *Chem. Phys.* **1996**, *221*, 147−161.

(60) Chong, D. P.; Aplincourt, P.; Bureau, C. *J. Phys. Chem. A* **2002**, *106*, 356−362.

(61) Gu, J.; Leszczynski, J. *J. Phys. Chem. A* **2000**, *104*, 6308−6313.

(62) Šponer, J.; Leszczynski, J.; Hobza, P. *Biopolymers* **2001**, *61*.

(63) Nir, E.; Plutzer, C.; Kleinermanns, K.; de Vries, M. *Eur. Phys. J. D* **2002**, *20*, 317−329.

(64) Nir, E.; Janzen, C.; Imhof, P.; Kleinermanns, K.; de Vries, M. S. *J. Chem. Phys.* **2001**, *115*, 4604−4611.

(65) Nir, E.; Kleinermanns, K.; de Vries, M. S. *Nature* **2000**, *408*, 949−951.

(66) Weinkauf, R.; Schermann, J. P.; de Vries, M. S.; Kleinermanns, K. *Eur. Phys. J. D* **2002**, *20*, 309−316.

(67) Desfrancois, C.; Abdoulcarime, H.; Schulz, C. P.; Schermann, J. P. *Science* **1995**, *269*, 1707−1709.

(68) Desfrancois, C.; Carles, S.; Schermann, J. P. *Chem. Rev.* **2000**, *100*, 3943−3962.

(69) Shelkovsky, V. S.; Stepanian, S. G.; Galetich, I. K.; Kosevich, M. V.; Adamowicz, L. *Eur. Phys. J. D* **2002**, *20*, 421−430.
(70) Chin, W.; Mons, M.; Dimicoli, I.; Piuzzi, F.; Tardivel, B.; Elhanine, M. *Eur. Phys. J. D* **2002**, *20*, 347−355.
(71) Dong, F.; Miller, R. E. *Science* **2002**, *298*, 1227−1230.
(72) Gidden, J.; Bowers, M. T. *Eur. Phys. J. D* **2002**, *20*, 409−419.
(73) Gutowski, M.; Dabkowska, I.; Rak, J.; Xu, S.; Nilles, J. M.; Radisic, D.; Bowen, K. H. *Eur. Phys. J. D* **2002**, *20*, 431−439.
(74) Gabelica, V.; De Pauw, E. *Int. J. Mass Spectrom.* **2002**, *219*, 151−159.